Switch of the Lowest Excited-States of Terpyridylplatinum(II) Acetylide Complexes Bearing Amino or Azacrown Moieties by Proton and Cations

Qing-Zheng Yang,[a] Qing-Xiao Tong,[a] Li-Zhu Wu,*[a] Zi-Xin Wu,[a] Li-Ping Zhang,[a] and Chen-Ho Tung*[a]

Keywords: Crown compounds / N ligands / Platinum / Sensors

The investigation of the synthesis and unique photophysical properties of two terpyridylplatinum(II) acetylide complexes [Pt(terpy)(C≡CC_6H_4-4-R)] where terpy is 2,2′:6′,2′′-terpyridyl and R = $N(CH_3)_2$ (**1**) or *N*-15-monoazacrown-5 (**2**) has been carried out. These complexes exhibit an absorption band in the region of 460–650 nm in neutral or basic solution that corresponds to a ligand-to-ligand charge transfer (LLCT) transition from the amino-substituted acetylide to the terpyridyl acceptor. In acidic solutions the complexes show the lowest-energy absorption band at 380–500 nm, which is assignable to a dπ(Pt)→π*(terpy) metal-to-ligand charge transfer (MLCT) transition. In acidic media the complexes are emissive with quantum yields of 1×10^{-3} to 2×10^{-3}, and lifetimes of 20–50 ns. Compound **2** may complex metal cations through its azacrown ether moiety. For Na^+, Ba^{2+}, Ca^{2+} and Mg^{2+}, a 1:1 binding mode with log *K*s of 2.52 to 4.18 was observed. As in the case of acidic solution, the cation-bound complex also features the lowest-lying MLCT excited state.

Introduction

The creation of host molecules that can selectively recognize specific guest molecules at their receptor site and produce a measurable physical change has been the subject of intense study.[1,2] Of particular interest is the design of molecules that show dramatic and reversible changes in color and/or luminescence in the visible spectral region upon exposure to specific substrates.[3−6] In this context square-planar platinum(II) complexes show considerable promise due to their rich and medium-sensitive spectroscopic and photophysical behavior.[7−10] In particular, alkynyl complexes of platinum(II) have received much attention because these complexes generally display bright luminescence with high quantum yields and long lifetimes, and a number of excellent studies have been performed.[11−23] Che and co-workers[11] reported a luminescent platinum(II) acetylide complex with aromatic diimine ligands in 1994. The [Pt(C≡CPh)$_2$(phen)] (phen = 1,10-phenanthroline) complex exhibits intense emission in fluid solution at room temperature, which was attributed to a triplet metal-to-ligand charge transfer [^{3}MLCT: dπ(Pt) → π*(phen)] excited state. Later on, Eisenberg and co-workers,[12−14] and Schanze and co-workers[15] investigated the excited-state properties of a series of complexes of the type [Pt(C≡C−Ar)$_2$(diimine)], where diimine is a series of 2,2′-bipyridine or 1,10-phenanthroline ligands and C≡C−Ar is a series of substituted arylacetylide ligands. They systematically examined the influence of the electronic demand of the diimine and arylacetylide ligands on the properties of the MLCT excited state, and revealed that in most cases the photophysics of the complexes is dominated by the energetically low-lying dπ(Pt) → π*(diimine) ^{3}MLCT state. Some of the complexes also feature a low-lying triplet intraligand (^{3}IL) ππ* excited state that is derived from transitions between π-type orbitals localized largely on the arylacetylide ligands.[16] Recently, Che and co-workers have used diiminepalatinum(II) bis(arylacetylide) complexes as emitters in organic light-emitting devices.[17,18]

The photoluminescence of [*trans*-Pt(C≡CR)$_2$](PEt_3)$_2$, where R = H or phenyl, in the solid state and frozen glass solution at 77 K was investigated by Demas and co-workers.[19] The emission was assigned as arising from a charge transfer excited state involving Pt d_{z^2} and acetylide π* orbitals. Yam and co-workers reported the luminescence of branched alkynylplatinum(II) complexes containing the [PtCl(C≡CC_6H_4C≡C)(PEt_3)$_2$] moiety, and suggested that the emission originates from a mixed π → π* (C≡CR) intraligand (IL)/$d_{z(Pt)}$ → π* (C≡CR) MLCT triplet state with predominantly IL character.[20] The photophysics of terpyridylplatinum(II) acetylide complexes and tridentate cyclometalated platinum(II) complexes bearing σ-alkynyl ligands was also reported.[21−23] Yam and co-workers investigated the photophysics and electrochemistry of a series of terpyridylplatinum(II) acetylide complexes with the general for-

[a] Technical Institute of Physics and Chemistry, the Chinese Academy of Sciences,
Beijing 100101, P. R. China
Fax: (internat.) +86-10-6487-9375
E-mail: chtung@mail.ipc.ac.cn
lzwu@mail.ipc.ac.cn

  DOI: 10.1002/ejic.200300878

mula $[Pt(C{\equiv}CC_6H_4R)(terpy)]PF_6$, and found that the emission energies depend on the nature of the acetylide ligands with different substituents on the phenyl ring:[21] an electron-withdrawing group on the phenyl ring increases the emission energy. Our laboratory has reported the photoluminescence of a series of 4′-*p*-tolyl-terpyridylplatinum(II) acetylide complexes.[22] These complexes exhibit long-lived emission from the ^{3}MLCT states with high emission quantum yields. The complexes bearing (C≡CR) ligands with R = alkyl in dichloromethane solution at room temperature show lifetimes greater than 10 μs and emission quantum yields greater than 0.25. We found that the cyclometalated platinum(II) complexes [Pt(C^N^N)(C≡CC_6H_4R)] where HC^N^N = 6-phenyl-4-*p*-tolyl-2,2′-bipyridine, also show photoluminescence with long lifetimes.[23]

Although the spectroscopic properties of alkynylplatinum(II) complexes have been extensively studied,[11−23] the utilization of such complexes for applications in molecular recognition and chemosensing work is rare.[21] In this paper we describe the syntheses and unique photophysical properties of two terpyridylplatinum(II) acetylide complexes [Pt(C≡ CC_6H_4-4-R)(terpy)] where R = $N(CH_3)_2$ (**1**) or *N*-15-monoazacrown-5 (**2**; Scheme 1). The amino groups in these complexes serve as proton receptors. In neutral or basic solutions, **1** and **2** are non-emissive and their low-energy absorption arises from a ligand-to-ligand charge transfer (LLCT) transition from the amino-substituted acetylide to the terpyridyl acceptor with a deep purple color. Upon protonation, these complexes display luminescence and their MLCT dπ→ π*(terpy) transition becomes the lowest energy absorption and the solutions are yellow in color. Thus, these complexes can be utilized as a chemosensor for proton detection by monitoring the changes both in luminescence and color. Significantly, the azacrown moiety in complexes **2** can also serve as metal-ion receptor. Upon complexing a metal cation, its ^{1}LLCT excited state shifts energetically to be above the ^{1}MLCT excited state, hence producing color changes from deep purple to yellow. Thus, **2** can also be employed as a chemosensor for the detection of metal ions. To the best of our knowledge, this is the first example to use the switch of the lowest excited state from the ^{3}LLCT to the ^{3}MLCT state of metal complexes for chemosensors.

Results and Discussion

Synthesis

The synthetic strategy for making the terpyridylplatinum(II) acetylide complexes is based on a CuI-catalyzed chloride-to-acetylide metathesis. Complexes **1** and **2** were prepared by reaction of [PtCl(terpy)]Cl with two equivalents of 4-(dimethylamino)phenylacetylene and 4-ethynylphenyl-*N*-15-monoazacrown-5 ether, respectively, in DMF in the presence of CuI and triethylamine at room temperature. After the metathesis reaction with KBF_4 for **1** or $LiClO_4$ for **2**, and recrystallization of the crude products by vapor diffusion of diethyl ether into an acetonitrile solution, **1** and **2** were obtained as dark-blue crystals in 70−76% yield. The identity of complexes **1** and **2** was confirmed by ^{1}H NMR spectroscopy, MS spectrometry and satisfactory elemental analyses. For comparison, the complex [Pt(C≡CC_6H_5)(terpy)]ClO_4 (**3**; Scheme 1) was also synthesized by a similar procedure.

Crystal Structure of Complex 1

A dark-blue single-crystal of dimensions 0.05 × 0.2 × 0.5 mm^3 in a glass capillary was used for data collection at 296 K on a Bruker Smart1000 X-ray diffractometer. The molecular structure and perspective drawing of the complex are depicted in Figure 1. The crystal belongs to the triclinic crystal system of centrosymmetric space group $P\bar{1}$ with unit cell parameters of a = 9.4033(8) Å, b = 11.0229(10) Å, c = 12.4015(11) Å; α = 101.619(2)°, β = 106.128(2)°, γ = 103.441(2)°, Important bond lengths and angles are given in Table 1. The coordination geometry about the platinum is essentially square planar with the bond from platinum to the central nitrogen atom of the terpyridine ligand slightly shorter than that to the other two outer nitrogen atoms, as is required by the steric demands of the terpyridine ligand. All the Pt−N distances are in the range found for typical platinum(II) terpyridine complexes.[21,28,29] The N−Pt−N angles [N(1)−Pt(1)−N(2): 80.59(17); N(2)−Pt(1)−N(3): 80.63(18); N(1)−Pt(1)−N(3): 161.18(19)] deviate from the idealized values of 90° and 180° as a consequence of the geometric constraints imposed by the terpyridyl ligands. The Pt−C bond length is 1.977 Å, which compares well with a value of 1.98 Å for other terpyridylplatinum(II) ace-

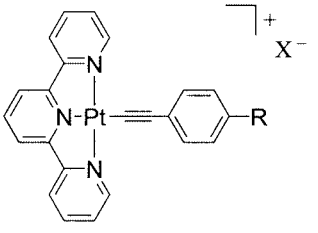

1. R = $N(CH_3)_2$ $X^- = BF_4^-$

2. R = 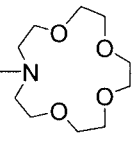 $X^- = ClO_4^-$

3. R = H $X^- = ClO_4^-$

Scheme 1

tylide complexes.[21] The C≡C bond length of 1.193 Å is similar to those of the other related platinum(II) acetylide complexes.[12,21,30] The phenyl ring of the acetylide ligand is almost coplanar to the platinum-terpyridine plane, with a dihedral angle of 4.5°. The crystal packing of **1** reveals a head-to-tail stacking between pairs of complex cations. The intermolecular Pt···Pt distance of 8.146 Å and the intermolecular separation of 6.718 Å between the terpy ligand and the phenyl group of the acetylide moiety are suggestive of a lack of intermolecular interactions between the metal centers and the aromatic groups.

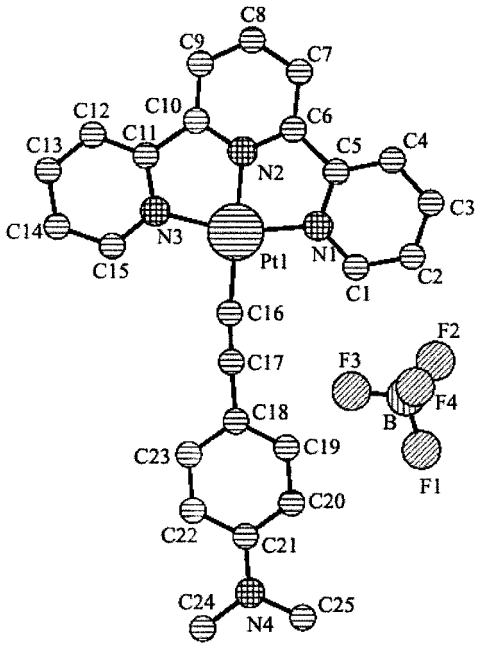

Figure 1. Perspective drawing of complex **1** with atomic numbering. (30% probability ellipsoids)

Table 1. Important bond lengths (Å) and bond angles (°) for complex **1**

Pt(1)−N(1)	2.004(4)	Pt(1)−N(2)	1.956(4)
Pt(1)−N(3)	2.014(5)	Pt(1)−C(16)	1.977(6)
C(16)−C(17)	1.193(8)	N(1)−Pt(1)−N(2)	80.59(17)
N(1)−Pt(1)−N(3)	161.18(19)	N(1)−Pt(1)−C(16)	98.3(2)
N(2)−Pt(1)−N(3)	80.63(18)	N(2)−Pt(1)−C(16)	178.00(19)
N(3)−Pt(1)−C(16)	100.5(2)	Pt(1)−C(16)−C(17)	173.7(5)

Absorption Spectra

Figure 2 presents the UV/Vis spectra of complexes **1** and **2** in acetonitrile solution. For comparison, the absorption spectrum of **3** is also shown in Figure 2. All the complexes exhibit intense vibronic-structured absorption bands at wavelengths below 350 nm, with extinction coefficients (ε) of the order of 10^4 $dm^3 \cdot mol^{-1} \cdot cm^{-1}$, and a less-intense band at 380−500 nm (centered at ca. 410, 411 and 432 nm with ε = 2860, 2950 and 4410 $dm^3 \cdot mol^{-1} \cdot cm^{-1}$ for **1**, **2** and **3** respectively). Significantly, complexes **1** and **2** show a moderately intense low-energy absorption band in the region of 460−650 nm (absorption maximum λ_{max} = 535 and 548 nm, ε = 4920 and 5370 $dm^3 \cdot mol^{-1} \cdot cm^{-1}$ for **1** and **2**, respectively). Complex **3** does not show such a band. The absorption spectral properties are found to follow Beer's Law at concentrations below 1×10^{-3} $mol \cdot dm^{-3}$, suggesting that no significant complex aggregation occurs. With reference to previous spectroscopic work on terpyridylplatinum(II) complexes,[21,22,31−34] the absorption bands at wavelengths below 350 nm are assigned to the intraligand (IL) transition of terpyridyl and acetylide ligands, while the absorption band at 380−500 nm is ascribed to the $d\pi(Pt) \rightarrow \pi^*$ (terpy) MLCT transition. The low-energy absorption band in the region of 460−650 nm for **1** and **2** is tentatively assigned to the LLCT transition from the amino-substituted acetylide ligand to the terpyridyl acceptor. This assignment is based on the following observations. First, the energy of the band increases with solvent polarity. For example, λ_{max} of the band for **1** is blue-shifted from 595 nm in dichloromethane to 535 nm in acetonitrile. This suggests that the ground state of the complex is more polar than its excited state, and is consistent with the notion that in the ground state the acetylide ligand is carbanionic in nature, and in the LLCT excited state the terpyridyl-acetylide ligands are like a diradical. Second, we have performed cyclic voltammetry studies on complexes **1** and **3** in acetonitrile. Both complexes exhibit two quasi-reversible cathodic waves in the potential region −0.8 to −1.5 V vs. SCE. By analogy to previous studies on other terpyridylplatinum(II) complexes,[21,22] these waves are ascribed to the reduction of the terpyridyl ligand with some mixing of the Pt^{II} character. Complex **3** displays an irreversible anodic wave with E_p at +1.22 V vs. SCE which has been assigned to a metal-centered oxidation from Pt^{II} to Pt^{III} by Yam and co-workers.[21] On the other hand, for complex **1** we observed an irreversible anodic wave near +0.63 V vs. SCE. Upon addition of an acid to the solution, this wave disappeared. Cyclic voltammetry of the uncomplexed ligand, *p*-(dimethylamino)-phenylacetylene exhibits a similar anodic wave at a slightly more positive potential (ca. +0.85 V vs. SCE). Thus, we

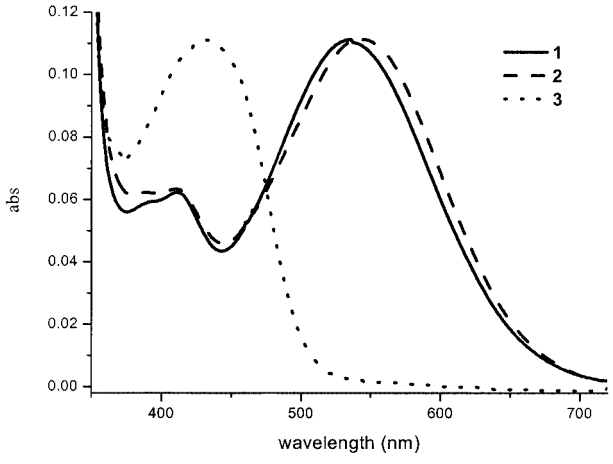

Figure 2. The normalized absorption spectra of complexes **1**−**3** in acetonitrile solutions at room temperature

assign the wave near +0.63 V to the oxidation of the amino-substituted acetylide ligand. Obviously, the LLCT transition in **1** should be at lower energy than the MLCT transition. Third, the lowest energy absorption band (λ_{max} = 535 and 548 nm) for **1** and **2** is red-shifted by more than 100 nm compared with that of **3** (λ_{max} = 432 nm). This observation is not consistent with the assignment of the 535 and 548 nm bands to a MLCT transition, because it has been established[12,21] that variation of the acetylide in platinum(II) acetylide complexes does not lead to very large changes in the Pt-based HOMO and the terpyridyl-based LUMO, hence it is not expected to affect the energy of the MLCT transition very much.

An Acid/Base-Controlled Molecular Switch based on Complexes 1 and 2

An initial observation when working with an acetonitrile solution of complex **1** was the change of the deep-purple color in neutral solution to yellow when exposed to a micromolar concentration of HBF_4. Such a dramatic color change, especially the large blue-shift of the absorption band in a dilute acidic medium, prompted an investigation of the nature of the acid-dependent absorption. Figure 3 shows the absorption spectra of complex **1** (3.87×10^{-5} mol·dm^{-3}) in acetonitrile as a function of added HBF_4. Upon addition of HBF_4 to the solution, the decrease in the absorption band at 535 nm is accompanied by a growth in the band with a maximum at 418 nm. Isosbestic points are observed at 457, 358, 344, 337 and 279 nm, indicative of the presence of only two absorbing species in the solution. The insert in Figure 3 shows a plot of the absorbance at 535 nm vs. the concentration of added HBF_4. Similar changes in the absorption spectrum were observed for complex **2** upon addition of HBF_4. In contrast, addition of HBF_4 to a solution of complex **3** in acetonitrile causes no marked changes in the absorption. These observations are evidently attributed to the protonation of the amino group in the acetylide ligands for complexes **1** and **2**. As the amino receptor is protonated in the presence of HBF_4, its electron-donating ability is decreased. This would dramatically lower the HOMO of the acetylide ligand. The Pt-based HOMO would also be lowered, but the extent of this lowering is expected to be much less than that of the acetylide ligand (Scheme 2). As a result, the LLCT transition from the amino-substituted acetylide ligand to the terpyridyl acceptor shifts to higher energy, and the dπ(Pt) → π*(terpy) MLCT transition becomes the lowest-energy transition.

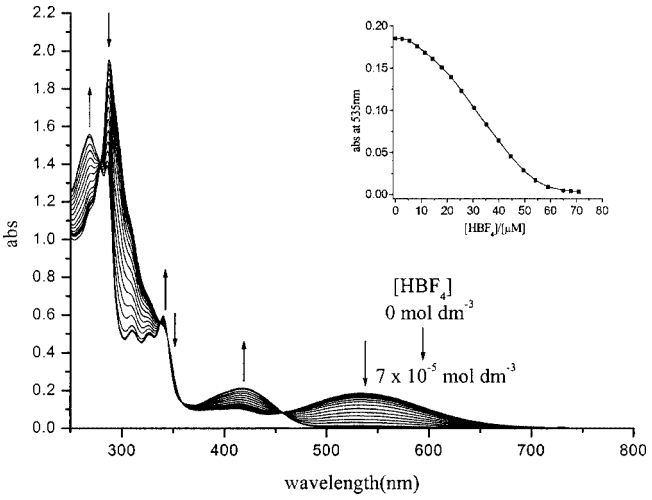

Figure 3. Absorption spectrum changes of complex **1** (3.87×10^{-5} mol·dm^{-3}) upon addition of various concentrations ($0-7 \times 10^{-5}$ mol·dm^{-3}) of HBF_4 in acetonitrile; the insert gives the titration curve for the plot of the absorbance at 535 nm vs. the concentration of HBF_4

The change in the luminescence response of complexes **1** and **2** towards protons was found to be even more pronounced. In neutral or basic solution **1** and **2** are non-emissive. The lack of emission upon excitation of the MLCT band is attributed to the transfer of the electron pair on the amino groups to the Pt^{III} metal center, resulting in an LLCT excited state. Because of the low energy, the ^{3}LLCT excited state decays via a non-radiative pathway. However, in acidic medium **1** and **2** exhibit a structureless emission band centered at about 560 nm. Figure 4 shows the change in the emission spectrum of **1** as a function of HBF_4 concentration. Throughout the titration, the excitation wavelength corresponds to the isosbestic point found at 457 nm in Figure 3. The emission intensity is noticeably

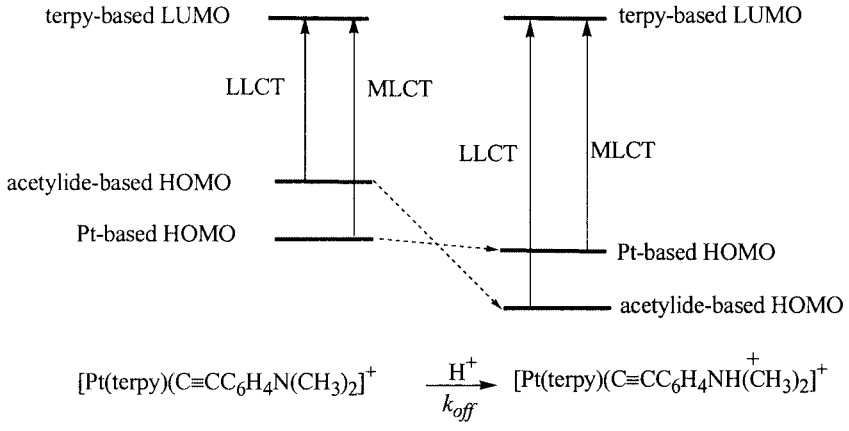

Scheme 2

enhanced upon increasing HBF_4 concentration, with saturation observed toward the end of the titration, while the shape and energy of the emission band remain unchanged. With reference to previous work on the emission of terpyridylplatinum(II) complexes,[21,22,29,31] this emission is assigned as being derived from the $d\pi(Pt)\rightarrow\pi^*$(terpy) ^{3}MLCT excited state. The insert in Figure 4 shows a plot of the emission intensity at 560 nm against the concentration of HBF_4. The emission quantum yields of **1** and **2** in their protonated form were measured to be 0.001 and 0.002, respectively, and their lifetimes 0.02 and 0.05 μs, respectively. Similar to the absorption studies, control experiments with complex **3** under the same conditions showed no change in the emission character upon addition of HBF_4. Evidently, the emission of complexes **1** and **2** upon addition of HBF_4 originates from protonation of the amino group. As mentioned above, upon protonation the ^{3}MLCT excited state becomes the lowest state and displays luminescence.

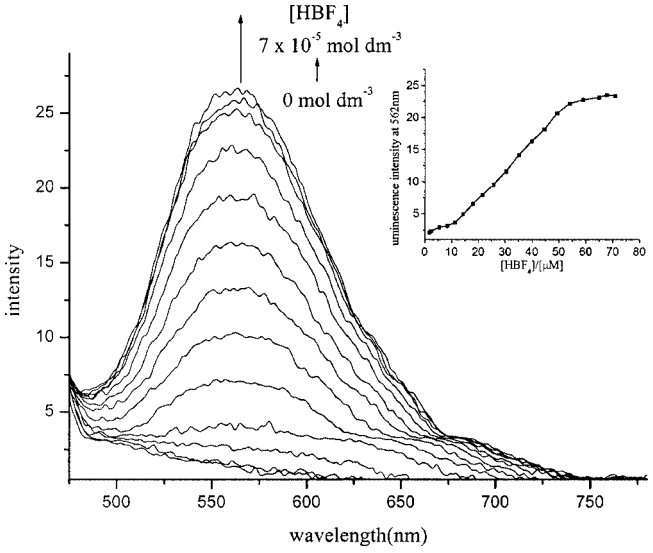

Figure 4. Luminescence spectrum changes of **1** (3.87×10^{-5} mol·dm^{-3}) upon addition of various concentrations ($0-7 \times 10^{-5}$ mol·dm^{-3}) of HBF_4 in acetonitrile; the insert shows the luminescence intensity at 560 nm as a function of HBF_4 concentration

The changes in absorption and emission behavior for complexes **1** and **2** are fully reversible. For example, subsequent addition of a base (e.g. triethylamine) to the acidic solution of **1** in acetonitrile led to the observation of a reverse trend: the luminescence was gradually quenched, and the absorbance at 418 nm dropped, with a concomitant rise in the absorption at 535 nm. Eventually the LLCT band in the absorption spectrum was totally recovered, and the solution became deep purple again. This result is indicative of the reversible nature of the protonation and deprotonation processes for the amino group in complexes **1** and **2**.

Cation-Binding Properties of Complex 2

Alkali and alkaline earth metal cations have profound effects on the absorption spectrum of **2**. Addition of Na^+, Ba^{2+}, Ca^{2+} or Mg^{2+}, as their perchlorate salts, to a solution of **2** in acetonitrile leads to dramatic changes in the absorption spectrum. Figure 5 presents the changes in the UV/Vis spectrum of **2** upon addition of Ca^{2+}. The lowest energy band at 548 nm decreases monotonically throughout the addition, while the band at 390−470 nm concomitantly grows-in with increasing Ca^{2+} concentration. Well-defined isosbestic points at 465, 375, 347, 342 and 283 nm were clearly observed. The solution becomes yellow at the end of the titration. Similar results were observed upon addition of other cations to the solution of **2**. This phenomenon evidently arises from the complexation of the cation with the azacrown ether receptor in the acetylide ligand, which decreases the electron-donating ability of the acetylide ligand, hence lowering the acetylide-based HOMO. Thus, the LLCT transition from the azacrown-containing acetylide ligand to the terpyridyl acceptor shifts to higher energy, and the $d\pi(Pt)\rightarrow\pi^*$(terpy) MLCT transition becomes the lowest energy absorption. Indeed, control experiments with the crown-free analogues **1** and **3** showed no such absorption spectrum changes upon addition of the cations under identical conditions. The insert in Figure 5 shows the plot of $A_0/(A_0 - A)$ vs. $[Ca^{2+}]^{-1}$, where A and A_0 refer to the absorbance at 548 nm for complex **2** in the presence and absence of Ca^{2+}, respectively. The straight line suggests that the complexation of the cation to the azacrown ether is in a 1:1 ratio. The bonding constants (log *K*s) determined from such plots for the cations are Na^+ (2.52), Ba^{2+} (3.01), Ca^{2+} (4.18) and Mg^{2+} (3.76), and their absolute values are very similar to those of other aza-15-crown-5 ionophores reported in the literature.[35]

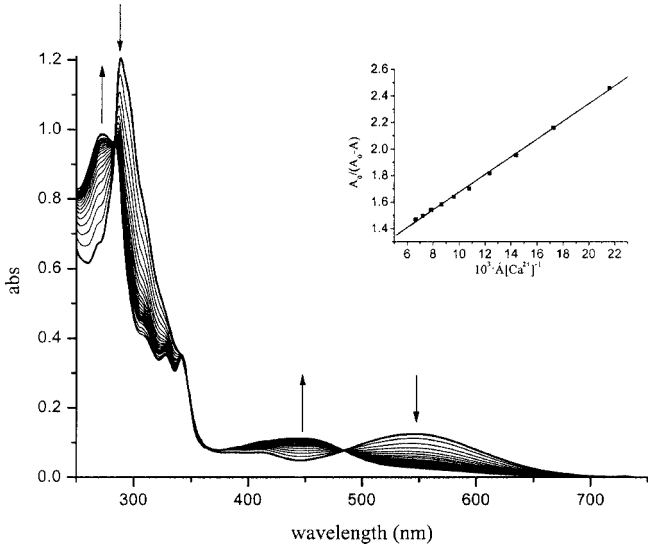

Figure 5. Absorption spectrum changes of **2** upon addition of various concentrations of Ca^{2+} in acetonitrile solution; the insert shows the plot of $A_0/(A_0 - A)$ vs. $[Ca^{2+}]^{-1}$

Complexation of cations with the azacrown ether receptor in **2** also affects the MLCT transition. We noted that the λ_{max} of the MLCT band of **2** complexed with the cations shifts to the blue side along the series Na^+ (481 nm),

Ba^{2+} (470 nm), Ca^{2+} (446 nm) and Mg^{2+} (430 nm). This reflects the difference in the strength of the ion-dipole interaction between the cations and the crown nitrogen. A strong interaction will further reduce the electron-donating ability of the acetylide and would make the metal center in **2** less electron-rich, and hence decrease the dπ(Pt)-orbital energy and cause the MLCT transition to occur at higher energy. It is well-known that the charge densities[36] of the metal ions increase in the following order: Na^+ (0.10) < Ba^{2+} (0.13) < Ca^{2+} (0.24) < Mg^{2+} (0.75). Mg^{2+} has the highest charge density in the series of metal ions studied in this work, and its value is considerably larger than the other cations. As a result, the interaction between Mg^{2+} and the crown nitrogen would be strongest, and complexation with this cation leads to the highest energy of the MLCT transition among the **2**·M^{n+} complexes.

In contrast to protonated **1** and **2**, complexation with metal cations does not cause luminescence from complex **2**, although the ^{3}MLCT state becomes the lowest energy excited state after complexation, as reflected in the absorption spectrum changes. This lack of emission may be interpreted by a kinetic model (Scheme 3) proposed by Schanze[37] for explanation of ion effect on the photophysics of a Re^I complex. In this scheme (N^N^N) and (C≡CPhAc) represent, respectively, the terpyridyl ligand and the acetylide with monoazacrown in complex **2**. Excitation of the **2**·M^{n+} complex produces the ^{1}MLCT state, which undergoes an intersystem crossing to the ^{3}MLCT state. Since the metal center in MLCT excited states (Pt^{III}) is much more electrophilic than that in the ground state (Pt^{II}), the charge density on the amino group will be reduced. This in turn decreases the binding ability of the azacrown, leading to the dissociation of the crown-complexed cation from the azacrown within the lifetime of the MLCT state. Thus, in addition to the normal radiative and non-radiative pathways, the ^{3}MLCT state of **2**·M^{n+} can also decay by a non-radiative pathway involving the dissociation of the crowned cation (k_{off}) followed by rapid internal conversion into the ^{3}LLCT state (k_{ic}). As a result, no emission could be detected from the acetonitrile solution of **2**·M^{n+}. The K_{off} values can be estimated by reference to the lifetime of the ^{3}MLCT state of protonated **2**. Assuming the deprotonation of **2**·H^+ in its ^{3}MLCT state is not competitive with the normal ^{3}MLCT decay rate, the lifetime (τ_1) of the ^{3}MLCT state of protonated **2** can be used to estimate the "normal" decay rate [$1/(k_r + k_{nr})$] of the ^{3}MLCT state of **2**·M^{n+}; k_{off} can then be obtained approximately from the lifetime (τ_2) of the ^{3}MLCT state of the **2**·M^{n+} complexes.

$$k_{off} = 1/\tau_2 - 1/\tau_1$$

The limiting value for the lifetime measurements in our instruments is > 0.2 ns, thus τ_2 for the complexes of **2** with cations is smaller than 0.2 ns. The emission lifetime (τ_1) of protonated **2** was measured to be 50 ns, as mentioned above. The k_{off} values obtained should therefore be greater than 5×10^9 s^{-1} for the cation-crowned complexes.

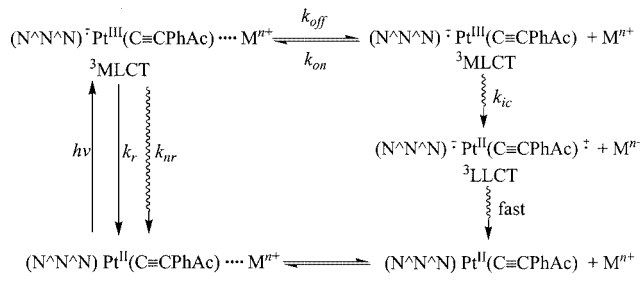

Scheme 3

Conclusion

Two terpyridylplatinum(II) acetylide complexes, one having an amino group and the other containing a monoazacrown moiety in their acetylide ligand, were prepared and their medium-sensitive photophysical properties were investigated. Incorporation of the amino or azacrown group into the acetylide destabilizes the HOMO of this ligand, hence in neutral or basic solutions the low-energy absorption of these complexes arises from the LLCT transition from the acetylide ligand to the terpyridyl acceptor. These complexes are non-emissive due to the fast non-radiative decay of the ^{3}LLCT excited state. Upon protonation of the amino group the HOMO of the acetylide ligand is lowered, thus the LLCT transition shifts to high energy, and the dπ(Pt)→π* (terpy) MLCT transition becomes the lowest energy absorption. In this case, the ^{3}MLCT state displays luminescence with a reasonably high quantum yield and long lifetime. Complexing a metal cation with the azacrown in complex **2** also results in a switch between the LLCT and MLCT transitions and dramatic absorption spectrum changes. The lack of emission for the cation-bound **2** is due to the dissociation of the crowned cation from the azacrown within the lifetime of the ^{3}MLCT state, and the rapid internal conversion from the ^{3}MLCT to the ^{3}LLCT states for the cation-free complex. These complexes can be utilized for molecular recognition and chemosensors specific for detection of proton and metal cations.

Experimental Section

Materials: 4-(Dimethylamino)phenylacetylene and [PtCl(terpy)]Cl·$2H_2O$ were prepared by literature methods.[24,25] 4-Ethynylphenyl-*N*-15-azacrown-5 ether was synthesized by a modified literature method.[24,26] Acetonitrile was distilled after refluxing for 3 h in the presence of P_2O_5. Other reagents were of analytical grade and used as received.

[Pt{C≡CC_6H_4-4-N$(CH_3)_2$}(terpy)]BF_4 (1): A mixture of [Pt(terpy)Cl]Cl·$2H_2O$ (100 mg, 0.19 mmol), CuI (10 mg), 4-(dimethylamino)phenylacetylene (55 mg, 0.38 mmol), 3 mL of DMF, and 4 mL of trimethylamine was sonicated under nitrogen for 8 h. An excess of an aqueous solution of KBF_4 was then added to the mixture. Dark-blue crystals were obtained after stirring for 1 h. The product was isolated, washed with water and diethyl ether. Subsequent recrystallization by diffusion of diethyl ether vapor into an acetonitrile solution of the product gave **1** as dark-blue crystals. Yield: 96 mg (76%). FAB-MS: *m/z* = 572 [M^+]. ^{1}H NMR ([D_6]DMSO): δ = 2.93 (s, 6 H), 6.68 (d, *J* = 8.4 Hz, 2 H), 7.34 (d,

J = 8.2 Hz, 2 H), 7.95 (t, J = 6.3 Hz, 2 H), 8.58 (m, 7 H), 9.21(d, J = 5.1 Hz, 2 H). $C_{25}H_{21}BF_4N_4Pt\cdot0.5H_2O$ (668.36): calcd. C 44.92, H 3.29, N 8.39; found C 44.87, H 3.59, N 8.58.

[Pt(C≡CC$_6$H$_4$-4-*N*-15-monoazacrown-5)(terpy)]ClO$_4$ (2): The synthesis of **2** was similar to that for complex **1**, except 4-ethynylphenyl-*N*-15-azacrown-5 ether was used in place of 4-(dimethylamino)phenylacetylene, and $LiClO_4$ was used in place of KBF_4. Yield: 110 mg (70%). FAB-MS: m/z = 746 [M^+]. ^{1}H NMR ([D$_6$]DMSO): δ = 3.64−3.82 (m, 20 H), 6.76 (d, J = 8.8 Hz, 2 H), 7.40 (d, J = 8.8 Hz, 2 H), 8.00 (t, J = 6.1 Hz, 2 H), 8.56−8.73 (m, 7 H), 9.16 (d, J = 5.1 Hz, 2 H). $C_{33}H_{35}ClN_4O_8Pt\cdot0.5H_2O$ (855.21): calcd. C 46.35, H 4.24, N 6.55; found C 46.32, H 4.18, N 6.15.

Physical Measurements and Instrumentation: UV/Vis spectra were obtained on a Shimadzu UV-1601PC spectrophotometer. Steady-state emission spectra were recorded on a Perkin Elmer LS50B spectrofluorometer. Elemental analysis was performed on a Carlo Erba 1106 elemental analyzer. ^{1}H NMR spectra were recorded on a Bruker-400 FT NMR spectrometer with chemical shifts (in ppm) relative to tetramethylsilane. FAB-MS spectra were run on a KYKY-ZHP mass spectrometer. X-ray analysis was performed on a Bruker Smart1000 X-ray diffractometer. Excited-state lifetimes were measured using a conventional laser system. The excitation source was the 355 nm line from the output of a Nd:YAG laser (third harmonic, 10 ns). All solutions were purged with argon for 15 min for emission spectra and lifetime measurements. The quantum yields of the emission were obtained by the optical dilute method using a degassed acetonitrile solution of $[Ru(bpy)_3](PF_6)_2$ as a reference (Φ = 0.062).[22] The ion-binding constants for **2** were calculated from the Hildebrand−Benesi equation: [27]

$$A_0/(A_0 - A) = A_0/\alpha[\text{complex } \mathbf{2}] + (A_0/\alpha[\text{complex } \mathbf{2}]\ Ks)\cdot(1/[M^{n+}])$$

where A and A_0 are the absorbance for complex **2** in the presence and absence of a metal ion, respectively, α is the ratio of complexation between complex **2** and the cation and Ks is the binding constant.

Crystallographic data for the structure reported in this paper have been deposited with the Cambridge Crystallographic Data Centre as supplementary publication No. CCDC-199962. Copies of the data can be obtained free of charge on application to CCDC, 12 Union Road, Cambridge CB2 1EZ, UK [Fax: (internat.) +44-1223/336-033; E-mail: deposit@ccdc.cam.ac.uk].

Acknowledgments

Financial support from the Ministry of Science and Technology of China (Grant Nos. G2000078104 and G2000077502) and the National Science Foundation of China (Nos. 20332040, 20333080, 20125207, 20272066, 20202013) is gratefully acknowledged. We also thank Dr. Jia-Hong Zhou for the cyclic voltammetry measurements, Prof. Wen Li for the emission lifetime measurements, and Prof. Ming Xiong and Mr. Guowu Li for the determination of the single crystal structure.

[1] J.-M. Lehn, *Supramolecular Chemistry, Concepts and Perspective*, VCH, Weinheim, **1995**.
[2] *Chemosensors of Ion and Molecular Recognition* (Eds.: J.-P. Desvergne, A. W. Czarnik), Kluwer, Dordrecht, **1997**, vol. 492.
[3] *Fluorescent Chemosensors for Ions and Molecule Recognition* (Ed.: A. W. Czarnik), Am. Chem. Soc., Washington DC, **1993**.
[4] A. P. de Silva, H. Q. Gunaratne, T. Gunnlaugsson, A. J. M. Huxley, C. P. McCoy, J. T. Rademacher, T. E. Rice, *Chem. Rev.* **1997**, *97*, 1515.
[5] D. H. Lee, J. H. Im, S. U. Son, Y. K. Chung, J.-I. Hong, *J. Am. Chem. Soc.* **2003**, *125*, 7752.
[6] M. S. Han, D. H. Kim, *Angew. Chem. Int. Ed.* **2002**, *41*, 3809.
[7] K. H. Wong, M. C. W. Chan, C. M. Che, *Chem. Eur. J.* **1999**, *5*, 2845.
[8] L.-Z. Wu, T. C. Cheung, C. M. Che, K. K. Cheung, M. H. W. Lam, *Chem. Commun.* **1998**, 1127.
[9] X.-H. Li, L.-Z. Wu, L.-P. Zhang, C.-H. Tung, C.-M. Che, *Chem. Commun.* **2001**, *21*, 2280.
[10] M. Kato, A. Omura, A. Toshikawa, S. Kishi, Y. Suginmoto, *Angew. Chem. Int. Ed.* **2002**, *41*, 3183.
[11] C.-W. Chan, L.-K. Cheng, C.-M. Che, *Coord. Chem. Rev.* **1994**, *132*, 87.
[12] M. Hissler, W. B. Connick, D. K. Geiger, J. E. McGarrah, D. Lipa, R. J. Lachiocotte, R. Eisenberg, *Inorg. Chem.* **2000**, *39*, 447.
[13] M. Hissler, J. E. McGarrah, W. B. Connick, D. K. Geiger, S. D. Cummings, R. Eisenberg, *Coord. Chem. Rev.* **2000**, *208*, 115.
[14] J. E. McGarrah, Y.-J. Kim, M. Hissler, R. Eisenberg, *Inorg. Chem.* **2001**, *40*, 4510.
[15] C. E. Whittle, J. A. Weinstein, M. W. George, K. S. Schanze, *Inorg. Chem.* **2001**, *40*, 4053.
[16] I. E. Pomestchenko, C. R. Luman, M. Hissler, R. Ziessel, F. N. Castellano, *Inorg. Chem.* **2003**, *42*, 1394.
[17] S.-C. Chan, M. C. W. Chan, Y. Wang, C.-M. Che, K.-K. Cheung, N. Zhu, *Chem. Eur. J.* **2001**, *7*, 4180.
[18] W. Lu, B.-X. Mi, M. C. W. Chan, Z. Hui, N. Zhu, S.-T. Lee, C.-M. Che, *Chem. Commun.* **2002**, 206.
[19] L. Sacksteder, E. Baralt, B. A. Degraff, C. M. Lukehart, J. N. Demas, *Inorg. Chem.* **1991**, *30*, 2468.
[20] V. W. W. Yam, C. H. Tao, L. Zhang, C. M. C. Wong, K. K. Cheung, *Organometallics* **2001**, *20*, 453.
[21] V. W.-W. Yam, R. P. L. Tang, K. M. C. Wong, K. K. Cheung, *Organometallics* **2001**, *20*, 4476.
[22] Q.-Z. Yang, L.-Z. Wu, Z.-X. Wu, L.-P. Zhang, C.-H. Tung, *Inorg. Chem.* **2002**, *41*, 5653.
[23] Z.-X. Wu, L.-Z. Wu, Q.-Z. Yang, L.-P. Zhang, C.-H. Tung, *Chin. J. Chem.* **2003**, *21*, 196.
[24] K. A. Leonard, M. I. Nelen, L. T. Anderson, S. L. Gibson, R. Hilf, M. R. Detty, *J. Med. Chem.* **1999**, *42*, 3942.
[25] M. Howe-Grant, S. J. Lippard, *Inorg. Synth.* **1980**, *20*, 101.
[26] C.-T. Chen, W.-P. Huang, *J. Am. Chem. Soc.* **2002**, *124*, 6246 and references cited therein.
[27] H. A. Benesi, J. H. Hildebrand, *J. Am. Chem. Soc.* **1949**, *71*, 2703.
[28] B. C. Tzeng, W. F. Fu, C. M. Che, H. Y. Chao, K. K. Cheung, S. M. Peng, *J. Chem. Soc., Dalton Trans.* **1999**, 1017.
[29] S. W. Lai, M. C. W. Chan, K. K. Cheung, C.-M. Che, *Inorg. Chem.* **1999**, *38*, 4262.
[30] C. J. Adams, S. L. James, X. Liu, P. R. Raithby, L. J. Yellowless, *J. Chem. Soc., Dalton Trans.* **2000**, 63.
[31] T. K. Aldridge, E. M. Stacy, D. R. McMillin, *Inorg. Chem.* **1994**, *33*, 722.
[32] J. A. Bailey, G. M. Hill, R. E. Marsh, V. M. Miskowski, W. P. Schaefer, H. B. Gray, *Inorg. Chem.* **1995**, *34*, 4591.
[33] G. Arena, G. Calogero, S. Campagna, L. M. Scolaro, V. Ricevuto, R. Romeo, *Inorg. Chem.* **1998**, *37*, 2763.
[34] D. R. McMillin, J. J. Moore, *Coord. Chem. Rev.* **2002**, *229*, 113.
[35] W. Burgermeister, R. Winkler-Oswatitsch, *Top. Curr. Chem.* **1977**, *69*, 91.
[36] The charge density (ρ) is defined as the amount of electronic charge per unit volume. It is given here by $\rho = g/(4/3\ \pi\ r^3)$ where g is the formal charge (+1 or +2) and r is the Shannon ion radius. The following values of r (Å) were used: Na^+ (1.32), Mg^{2+} (0.86), Ca^{2+} (1.26), Ba^{2+} (1.56): R. D. Shannon, *Acta Crystallogr.* **1976**, *32*, 751.
[37] D. B. MacQueen, K. S. Schanze, *J. Am. Chem. Soc.* **1991**, *113*, 6108.

Received November 17, 2003
Early View Article
Published Online March 30, 2004

